Pergamon

Int. J. Heat Mass Transfer. Vol. 40, No. 10, pp. 2407–2417, 1997

0017–9310/97 $17.00+0.00

PII: S0017–9310(96)00287–6

Mathematical modelling of the performance of non-isothermal membrane reactors

M. K. KOUKOU, G. CHALOULOU, N. PAPAYANNAKOS and N. C. MARKATOS†

National Technical University of Athens, Department of Chemical Engineering, 9, Heroon Polytechniou Str., GR-157 80, Athens, Greece

(*Received* 21 *September* 1995 *and in final form* 26 *July* 1996)

Abstract—The development of a mathematical model is presented, which simulates the performance of a non-isothermal packed-bed membrane reactor. The model takes into account the various heat exchanges that take place inside the reactor. A set of partial-differential conservation equations, coupled with the appropriate boundary and internal conditions describing the physical problem considered is solved, using finite-volume techniques. In this study, the developed mathematical model is applied to investigate the endothermic dehydrogenation of cyclohexane in a packed-bed membrane reactor, where a permselective porous glass membrane is embodied. It is shown that the assumption of isothermal conditions, or even the omission of certain thermal phenomena that take place inside the reactor, lead to a significant overestimation of the predicted temperature field and of the membrane reactor conversion.

1. INTRODUCTION

The majority of chemical reactions do not reach complete conversion of the reactants, but, in general, they reach an equilibrium conversion below 100%. The shift of conversion beyond its value at equilibrium can be achieved by continuous removal of the reaction products with membrane reactors, a modern technology that has been of growing interest lately. Besides the experimental work, some efforts have been reported concerning the numerical simulation of the process. In most of these, the mass and components balances have been successfully solved. However, in most cases the problem of heat balance has not been realistically described. The majority of the reported studies assume isothermal conditions inside the reactor [1–3], neglect the effect of radial and axial heat dispersion [4] and suppose that the resistance to heat transfer between the membrane wall and the fluid is negligible [2]. These assumptions may lead to unrealistic simulation of the reactor operation.

The objective of the present study is to develop a numerical code for the simulation of the performance of a packed-bed membrane reactor, under non-isothermal conditions; and to investigate the thermal effects on reactor simulation. This has been achieved by the development of a two-dimensional mathematical model which simulates the flow, chemical reaction and separation through the membrane taking into account the various heat phenomena that take place inside the reactor.

Two operation modes are studied: (i) adiabatic operation; and (ii) non-adiabatic operation, where the outer wall of the reactor remains at a constant temperature. A comparison is also made with the performance of a membrane reactor operating isothermally. Two further cases are finally studied, one with heat dispersion conditions and the other with heat dispersion free conditions on both sides of the reactor.

2. DESCRIPTION OF THE MATHEMATICAL MODEL

2.1. *Posing the physical problem*

The analysis of the physical problem is presented in this section according to which the mathematical model was developed. The membrane reactor is considered as an annulus, divided into two compartments: (i) the inner tube (feed side), formed by the membrane and packed with a catalyst, where a gas mixture is fed to and the reaction takes place; and (ii) the free space between the two tubes (separation side) where a sweep gas is fed to, being enriched with the separated gases all the way to the outlet (permeate stream) (Fig. 1(a)). Inside the membrane reactor and especially in the area close to the membrane the following heat effects may be important and are all taken into account (Fig. 2, Table 1): (i) enthalpy input by the two gas streams; (ii) consumption of heat by the endothermic reaction; (iii) heat transfer through the membrane by conduction and by the diffusion of molecules passing through the membrane; (iv) heat transmission between the membrane walls (and the outer tube wall, when non-adiabatic conditions are considered) and the fluid in contact; (v) simultaneous heat dispersion within the two separate parts of the reactor.

† Author to whom correspondence should be addressed.

NOMENCLATURE

A heat exchange area [m^2]
C_p specific heat of the fluid [J kg^{-1} K^{-1}]
d_e equivalent diameter [m]
d_p particle diameter [m]
D_2 is the diameter of the feed side + the membrane layer [m]
D_3 is the total diameter of the reactor [m]
D_h $= D_3 - D_2$
D_r radial diffusion coefficient [m^2 s^{-1}]
D_z axial diffusion coefficient [m^2 s^{-1}]
D_ϕ mass dispersion coefficient [m^2 s^{-1}]
F_m total permeation rate through the membrane [kg s^{-1}]
Gr Grashof number
h_s, h_f coefficients of heat transmission between the membrane surface and the fluid on separation side and feed side, respectively [W m^{-2} K^{-1}]
h'_s coefficient of heat transmission between the external reactor wall and the fluid on the separation side [W m^{-2} K^{-1}]
H_{memf} specific enthalpies of the mixture
H_{mems} passing through the membrane material calculated at membrane wall temperatures on the feed side and separation side, respectively [J kg^{-1}]
k membrane thermal conductivity [W m^{-1} K^{-1}]
k_C constant of rate equation [mol m^{-3} Pa^{-1} s^{-1}]
K_B constant of rate equation [Pa^{-1}]
K_P constant of rate equation [Pa^3]
l_o reactor length [m]
L length of packed column [m]
M_i molecular weights of the components [kg $gmol^{-1}$]
MW mixture mean molecular weight [kg $gmol^{-1}$]
Nu Nusselt number
P_f total pressure on the feed side [Pa]
P_s total pressure on the separation side [Pa]
Q_f inlet feed rate [kg m^{-2} s^{-1}]
Q_s inlet sweep gas rate [kg m^{-2} s^{-1}]
Q_i separation rate of component i [kg m^{-2} s^{-1}]
Q_{h1} transmission rate of heat from the fluid on the separation side to the outer surface of the membrane [J s^{-1}]
Q_{m1} rate of enthalpy input to the separation side by the molecules passing through the membrane [J s^{-1}]
Q_{cond} rate of heat conduction through the membrane [J s^{-1}]
Q_{h2} transmission rate of heat from the inner surface of the membrane to the fluid on the feed side [J s^{-1}]
Q_{m2} rate of heat output by the molecules passing through the membrane and leaving the feed side [J s^{-1}]
r reaction rate [mol m^{-3} s^{-1}]
r_{out} outer radius of reactor [m]
R_1, R_2 inner and outer membrane tube radii, respectively [m]
Re $(= d_e u/v)$ Reynolds number
Re_{D_h} is the Reynolds number corresponding to equivalent diameter D_h
T absolute temperature [K]
T_f, T_s fluid temperature near the wall on the feed side and separation side, respectively [K]
T_{memf} wall temperatures on the feed side and
T_{mems} separation side respectively [K]
$u_{C,i}$ cyclohexane at feed side inlet [molC_6H_{12} s^{-1}]
$u_{C,o}$ cyclohexane at feed side outlet [molC_6H_{12} s^{-1}]
$v_{C,o}$ cyclohexane at separation side outlet [molC_6H_{12} s^{-1}]
$\bar{v}$ velocity vector
v_s superficial velocity, $v_s = v \cdot \varepsilon$ [mol s^{-1}] where v is the interstitial velocity
V feed side volume [m^3]
x_i molar fraction of the component i on the feed side
y_i molar fraction of the component i on the separation side
X membrane reactor conversion.

Greek symbols

α_i permeability coefficient [kg m^{-2} s^{-1} Pa^{-1}]
Γ_ϕ effective exchange coefficient of ϕ [kg m^{-1} s^{-1}]
ΔH heat of the reaction [J mol $C_6H_{12}^{-1}$]
ε bed porosity
λ_g heat conduction coefficient of the fluid [W m^{-1} K^{-1}]
λ_{af} axial effective heat dispersion coefficient on the feed side [W m^{-1} K^{-1}]
λ_{as} axial effective heat dispersion coefficient of the fluid on the separation side [W m^{-1} K^{-1}]
λ_{rf} radial effective heat dispersion ceofficient on the feed side [W m^{-1} K^{-1}]
λ_{rs} radial effective heat dispersion coefficient of the fluid on the separation side [W m^{-1} K^{-1}]
μ laminar viscosity [Pa s^{-1}]
ν kinematic viscosity [m^2 s^{-1}]
ρ density of the mixture [kg m^{-3}]
ϕ dependent variable [units ϕ]
ϕ_z (=l/lo), dimensionless reactor length
ϕ_R (=r/rout), dimensionless radius.

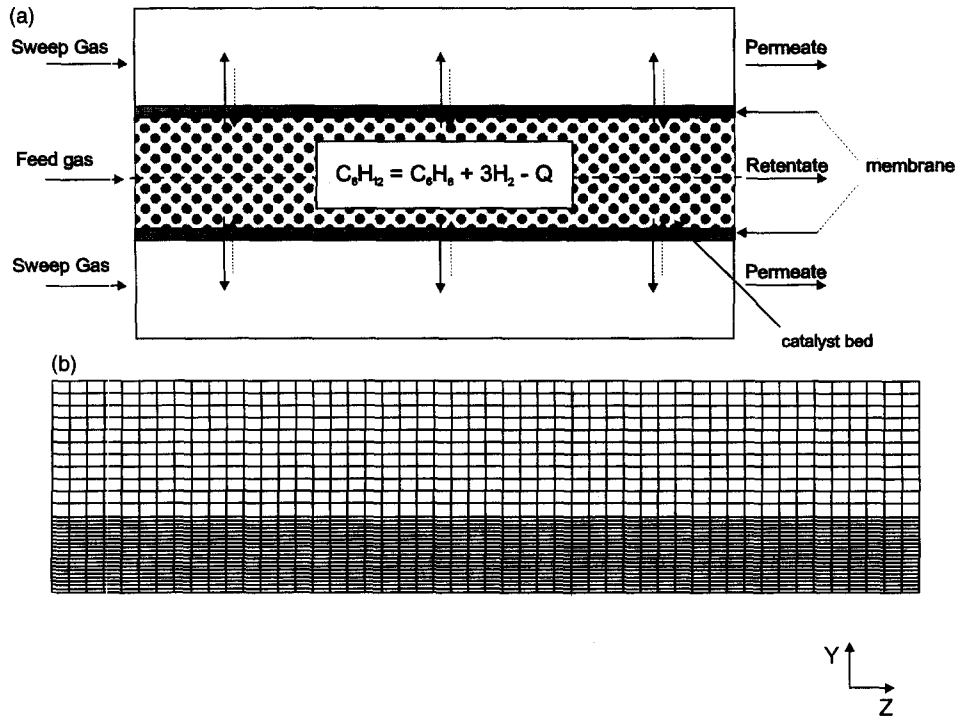

Fig. 1. (a) Representation of the physical problem considered; (b) typical numerical grid (31 × 50) used in the simulation.

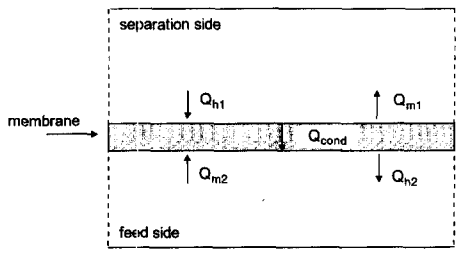

Fig. 2. Representation of the heat fluxes in the area close to the membrane.

2.2. *Model development*

2.2.1. *Mathematical formulation.* A two-dimensional, single-phase mathematical model is considered which simulates the flow, chemical reaction and separation through the membrane, taking into account the heat effects that take place inside the reactor. The model is considered two-dimensional because both mass and energy flow not only in the direction of the bulk flow, but also in the vertical direction.

The main assumptions made for the application presented in this work are:

- Plug flow of mass on both sides of the reactor.
- Steady-state operation.
- The permeabilities of the components passing through the membrane were considered independent of temperature for the temperature range studied.
- Co-current flow of sweep and feed gas.
- Atmospheric pressure conditions.

Forming the heat balance equation in the neighbourhood of the membrane and assuming that the temperature on the separation side is greater than the temperature on the feed side (which is generally the case when the two fluid streams enter at equal temperatures), the general form of the heat balance is (Fig. 2, Table 1):

$$Q_{h1} + Q_{m1} = Q_{cond} = Q_{h2} + Q_{m2} \qquad (1)$$

where:

Q_{h1} transmission rate of heat from the fluid on the separation side to the outer surface of the membrane;

Q_{m1} rate of enthalpy input to the separation side by the molecules passing through the membrane;

Q_{cond} rate of heat conduction through the membrane;

Q_{h2} transmission rate of heat from the inner surface of the membrane to the fluid on the feed side;

Q_{m2} rate of heat output convected by the molecules passing through the membrane and leaving the feed side.

Conservation equations. The mathematical model developed in this study describes the balance of the relevant quantity (dependent variable), expressed by the following partial differential equation:

$$\partial \rho\phi/\partial t + \mathrm{div}(\rho \bar{v}\phi + \Gamma_\phi \,\mathrm{grad}\,\phi) = S_\phi. \qquad (2)$$

The dependent variable ϕ may be: the mixture pres-

Table 1. Expressions used to describe the heat balance inside the reactor and the area close to the membrane

• Heat consumption by the endothermic reaction

$$Q_{react} = rV\Delta H$$

r	reaction rate [mol m^{-3} s^{-1}]
V	feed side volume [m^3]
ΔH	heat of the reaction [J mol $C_6H_{12}^{-1}$].

• Transmission rate of heat between the membrane walls (and the outer tube wall, when non-adiabatic conditions are considered) and the fluid in contact

$$Q_{h1} = \pm h_s A(T_s - T_{mems}) \quad Q_{h2} = \pm h_f A(T_f - T_{memf})$$

h_s, h_f	heat transfer coefficients between the membrane surface and the fluid on separation side and feed side respectively [W m^{-2} K^{-1}]
A	heat exchange area [m^2]
T_f, T_s	fluid temperature near the wall on the feed side and separation side, respectively [K]
T_{memf}, T_{mems}	membrane wall temperatures on the feed side and separation side, respectively [K].

• Heat conduction rate through the membrane material.

$$Q_{cond} = k2\pi L(T_{mems} - T_{memf})/\ln(R_2/R_1)$$

k	membrane thermal conductivity [W m^{-1} K^{-1}]
L	reactor length [m]
R_1, R_2	inner and outer membrane tube radii, respectively, [m]
T_{memf}, T_{mems}	membrane wall temperatures on the feed side and separation side, respectively [K].

• Enthalpy transfer rate due to the molecules' motion through the membrane:

$$Q_{m1} = F_m \cdot H_{mems} \quad Q_{m2} = F_m \cdot H_{memf}$$

H_{memf}, H_{mems}	specific enthalpies of the mixture passing through the membrane material calculated at membrane wall temperatures on the feed side and separation side, respectively [J kg^{-1}]
F_m	total permeation rate through the membrane [kg s^{-1}]

sure P (N m^{-2}), the radial and axial velocity components v, w (m s^{-1}), the mass fractions of chemical species c_i (kg_i kg^{-1}) and the mixture specific enthalpy h (J kg^{-1}).

The term $\partial\rho\phi/\partial t$ is the unsteady-state contribution (in the particular problem its value is zero, as steady-state conditions are assumed). The term $\mathrm{div}(\rho\bar{v}\phi)$ expresses the transfer of the quantity ϕ due to convection with the fluid. The term $\mathrm{div}(\Gamma_\phi \,\mathrm{grad}\,\phi)$ expresses the transfer of ϕ due to diffusion. Finally, the term S_ϕ expresses the consumption or the production of ϕ inside the domain of interest. The exchange coefficient Γ_ϕ in the diffusion term, in the case of mass fraction equation, is equal to: $\Gamma_\phi = \rho D_\phi$ where D_ϕ is the mass dispersion coefficient. The plug-flow profile is achieved assuming that the radial dispersion coefficient is much greater than the axial one.

In the enthalpy equation, Γ_ϕ is equal to: $\Gamma_\phi = \lambda^{eff}/C_p$ (kg m^{-1} s^{-1}). In particular, heat is not only "diffused" inside the reactor (i.e. transmitted by conduction), but, in general, is "dispersed" (i.e. transmitted both by conduction and by other mechanisms, such as turbulence, mass diffusion, velocity gradients, etc.) and that is why the coefficient λ^{eff} is called "effective". Thermal dispersion is studied separately, according to whether it takes place in the longitudinal (axial) or the radial direction. The presence of axial thermal dispersion is indicative of the fact that heat is not only transferred by convection, but furthermore is transmitted by dispersion, whereas the presence of radial thermal dispersion indicates that the radial temperature profile is not uniform, due to resistances in the heat transmission radially. Both phenomena indicate that the assumption of plug conditions is not valid for heat.

Thermal dispersion on the separation side is attributed only to heat conduction within the fluid, because the low flow rates do not imply the appearance of turbulence, whereas other phenomena, such as mass diffusion, are considered negligible. Thus, the coefficient Γ_ϕ is substituted by the fluid mean thermal conductivity coefficient. On the feed side, where fluid and solid particles coexist, the situation becomes more complicated as heat dispersion is attributed to the conduction within the fluid and solid phase, the interphase influence and the effects of the fluid movement. All these can be described either separately (two-phase models [5, 6]) or combined to one effect (one-phase models [7, 8]). In the present case, a one-phase model was selected, giving the so-called "effective axial ther-

mal conduction coefficient", λ_{ax}^{eff} and the "effective radial thermal conduction coefficient" λ_{rad}^{eff}, describing the overall phenomena (Appendix 1).

In order to solve the set of conservation equations described previously it is necessary to provide adequate boundary and internal conditions for each of the equations solved, describing the physics of the problem examined. These conditions are discussed in the description of the application of the model.

2.2.2. *Numerical solution.* The solution procedure employed to solve the set of the conservation partial-differential equations along with the appropriate boundary-internal conditions embodies the SIMPLEST algorithm, and details on it are found in the literature [9–14]. The computational domain of interest is discretized into a number of finite control volumes (cells) and the differential equations for the various ϕs are integrated over them, providing the corresponding set of finite-domain equations. This set is solved numerically and yields values of the dependent variables at the centre of the computational cells. Concerning the calculation of the velocities, the conventional "staggered grid" arrangement is applied [10] to calculate them at the middle of the computational cell faces to which they are normal.

3. APPLICATION OF THE MODEL

3.1. *Geometrical details—numerical grid*

The membrane reactor geometry, which is a typical one for laboratory use [1–4], and the respective computational grid used in the modelling are illustrated in Fig. 1(a, b). The membrane is placed on the inner cylinder of the reactor and its dimensions are presented in Table 2. The catalyst bed is placed inside the inner tube. The calculations were done using cylindrical-polar coordinates, with a two-dimensional grid covering the region of interest and consisting of 31×50 cells in the radial r- and axial z-direction, respectively.

3.2. *Specification of boundary-internal conditions*

Boundary conditions. Inlet-Outlet. Inlet feed rates are specified for all dependent variables and for both sides of the computational domain. Typical ranges of the inlet flows and their compositions are shown in Table 3. At the outlet, the external pressure is considered equal to the atmospheric and the computed pressures in the computational domain are relative to it.

Table 2. Reactor dimensions and membrane characteristics used in the modelling

Reactor length [m]	0.391
Inner tube radius [m]	7.2×10^{-3}
Outer tube radius [m]	2.025×10^{-2}
Membrane thickness [m]	1.35×10^{-3}
Mean pore diameter [nm]	4.0
Void fraction	0.28
Thermal conductivity [17] [W m^{-1} K^{-1}]	1.7

Table 3. Inlet feed rates and compositions used in the modelling

	Inlet flux [kg m^{-2} s^{-1}]	Composition [w w^{-1}]
Feed side	7.5×10^{-3}–12.5×10^{-3}	34% C_6H_{12}, 66% Ar
Separation side	0.0–0.22	100% Ar

Wall friction. The no-slip condition is used for velocities and the fluid-to-wall friction losses are computed by the log-law functions at all walls [9].

Symmetry plane boundary. Zero-flux conditions are applied at the symmetry plane for all variables.

Internal conditions. Gas permeation equation. The permeation rate of the chemical species through the membrane material is calculated by equation (i) in Table 4. Permeability values are a function of temperature, but in this case, they are considered constant, because of the small temperature range studied. They are also a function of the nature of chemical component and of the size of its molecules. The overall permeation rate is the algebraic sum of the components rates.

Reaction kinetics. The expression used to describe the reaction rate of the dehydration of cyclohexane over catalyst Pt/Al_2O_3 was that of Itoh *et al.* [3], for the temperature range studied (T = 470–490 K) and it is shown in Table 4.

Momentum loss in packed bed. The well-known Ergun equation was used to describe the momentum loss in the packed bed, in terms of pressure gradient [15] as it is shown in Table 4.

3.3. *Calculation of thermal properties*

The formulation of the basic conservation equations, requires the calculation of thermal properties (e.g. thermal conductivities, heat transfer coefficients) given in Appendix 1.

3.4. *Overview of cases examined*

The developed numerical code was applied to study the following cases:

- Adiabatic packed-bed membrane reactor where: (i) heat dispersion effects were neglected on both sides of the reactor (simplified model); and (ii) heat dispersion effects were taken into account (heat dispersion model).
- Non-adiabatic packed-bed membrane reactor where the outer cylinder wall remained at a constant temperature and: (i) heat dispersion effects were neglected on both sides of the reactor; or (ii) heat dispersion effects were taken into account. This case corresponds to experiments where the isothermal

Table 4. Gas permeation equation (i), reaction kinetics (ii), catalyst characteristics (iii) and Ergun equation (iv) used in the modelling

(i) $Q_i = \alpha_i(x_i P_f - y_i P_s)$	Q_i	separation rate of component i	[kg m^{-2} s^{-1}]
	α_i	permeability coefficient of component i	[kg m^{-2} s^{-1} Pa^{-1}]
	x_i	molar fraction of the component i on the feed side	
	y_i	molar fraction of the component i on the separation side	
	P_f	total pressure on the feed side	[Pa]
	P_s	total pressure on the separation side.	[Pa]
(ii) $r = -\dfrac{k_C\left(K_P\dfrac{P_C}{P_H^3} - P_B\right)}{1 + K_B K_P \dfrac{P_C}{P_H^3}}$		$k_c = A1\exp(-4270/T)$	[mol m^{-3} Pa^{-1} s^{-1}]
		$K_B = 2.03\times10^{-10}\exp(6270/T)$	[Pa^{-1}]
		$K_P = 4.89\times10^{-5}\exp(-26490/T)$	[Pa^3]
		where $A1 = 0.221$	[mol m^{-3} Pa^{-1} s^{-1}]
		p_i, is the partial pressure of component i.	
(iii) Pt/Al_2O_3		0.5%	[w w^{-1}]
particle diameter		3.55×10^{-3}	[m]
bed porosity		0.38	
(iv) $\dfrac{\Delta p}{L} = 150\dfrac{(1-\varepsilon)^2\mu v_s}{\varepsilon^3 d_p^2} + 1.75\dfrac{(1-\varepsilon)v_s^2\rho}{\varepsilon^3 d_p}$			
	Δp	the pressure drop	[Pa]
	L	the length of the packed column	[m]
	ε	the void fraction equal to 0.38	
	μ	the laminar viscosity of the gaseous mixture	
	v_s	the superficial velocity which is equal to: $v_s = v\cdot\varepsilon$ and v is the interstitial velocity.	[m s^{-1}]

conditions in the reactor are controlled at the reactor outer tube surface.

- Isothermal operation.

3.5. *Computational details*

Runs were performed on a Silicon Graphics R4000 XS24 Indigo Workstation and convergence was easily obtained by applying relaxation of the false-time step type [11] in the mass fraction equations, and linear relaxation for the other variables. About 4500 sweeps of the computational domain were needed in order to obtain full convergence, using a grid of 31×50 and each sweep took about 2 s.

The choice of the computational grid used in the performed runs was related to the physical problem considered and it was selected finer on the feed side. The final choice was made performing independence runs as shown in Figs. 3 and 4, and the decision was based on a trade off between the computer time and the expected accuracy for a certain number of iterations. It is noted, that as reactor conversion did not essentially change using a grid finer than 31×50, the latter grid was adopted as the best one to be used in the simulation runs.

4. SIMULATION RESULTS AND DISCUSSION

In this section results from the application of the mathematical model, in terms of membrane reactor conversion, $X(X = \{1-(u_{C,o}+v_{C,o})/u_{C,i}\})$ and temperature profiles, are presented and discussed. The analysis is achieved by varying either the inlet rates or the inlet temperatures on both sides of the reactor.

In Figs. 5–12, it is easily remarked that the use of a packed-bed membrane reactor causes an important increase in reactor conversion in relation with that achieved in a conventional reactor for $Q_s = 0$ (2–8 times the conventional reactor conversion). It is also obvious, that: (i) an increase in inlet feed rate induces a decrease in reactor conversion; while (ii) an increase of the inlet sweep gas rate causes an increase in reactor conversion, until a maximum value of the latter is reached. In that case, the partial pressure difference of gases takes its maximum value.

In the numerical simulation of the performance of a membrane reactor, heat effects taking place inside the reactor (heat dispersion on both sides of the reactor, heat transfer through the membrane material, heat consumption from the endothermic reaction) have to be studied. Assuming isothermal conditions or even neglecting heat dispersion results leads to an overestimation of the calculated temperature field and, thus, an overestimation of the reactor conversion (Figs. 9–12).

High errors are observed when: (i) the heat of the reaction is neglected (Figs. 9–12) in the isothermal case; and (ii) heat dispersion effects either in radial or in axial direction are not taken into account (Figs. 5–8). On the separation side, it is observed that there is high resistance to the heat transfer from the fluid to

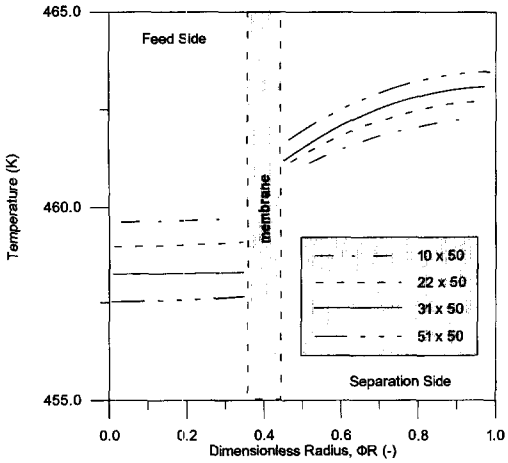

Fig. 3. Radial profile of temperature at $\phi_z = 0.5$, for various grids (NY × NZ). Adiabatic operation. $Q_f = 12.5 \times 10^{-3}$ kg·m^{-2}·s^{-1}, $Q_s = 6 \times 10^{-2}$ kg·m^{-2}·s^{-1}. Inlet temperature on both sides: $T = 470$ K. Heat dispersion model.

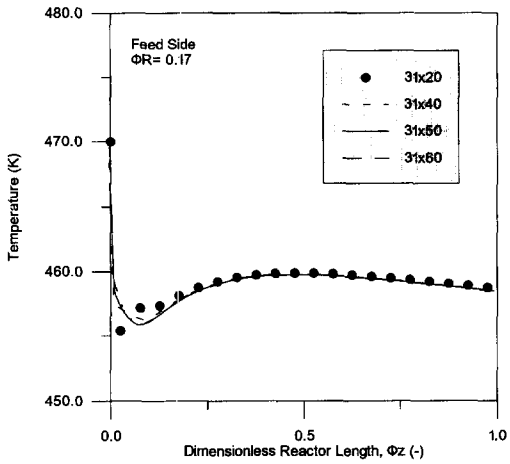

Fig. 4. Axial profile of temperature for various grids (NY × NZ). Adiabatic operation. $Q_f = 12.5 \times 10^{-3}$ kg·m^{-2}·s^{-1}, $Q_s = 6 \times 10^{-2}$ kg·m^{-2}·s^{-1}. Inlet temperature on both sides: $T = 470$ K. Simplified model.

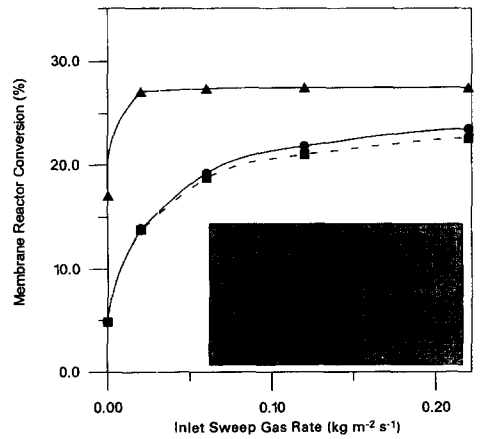

Fig. 5. Membrane reactor conversion vs inlet sweep gas rate. Inlet feed rate = 12.5×10^{-3} kg·m^{-2}·s^{-1}. Inlet temperature on both sides: $T = 470$ K.

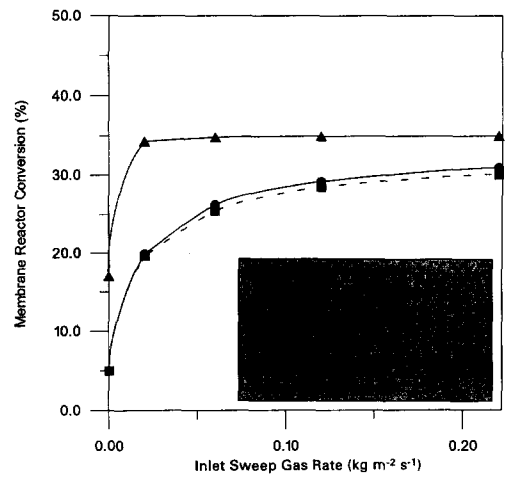

Fig. 6. Membrane reactor conversion vs inlet sweep gas rate. Inlet feed rate = 7.5×10^{-3} kg·m^{-2}·s^{-1}. Inlet temperature on both sides: $T = 470$ K.

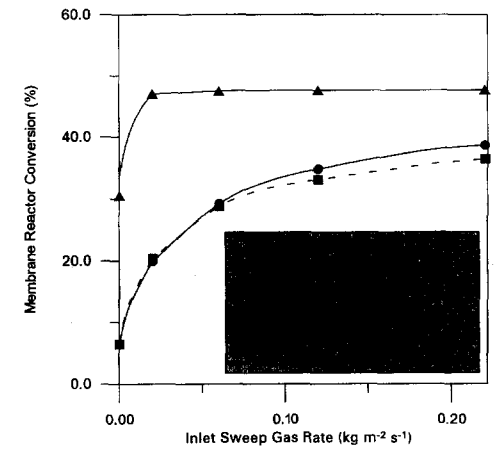

Fig. 7. Membrane reactor conversion vs inlet sweep gas rate. Inlet feed rate = 12.5×10^{-3} kg·m^{-2}·s^{-1}. Inlet temperature on both sides: $T = 490$ K.

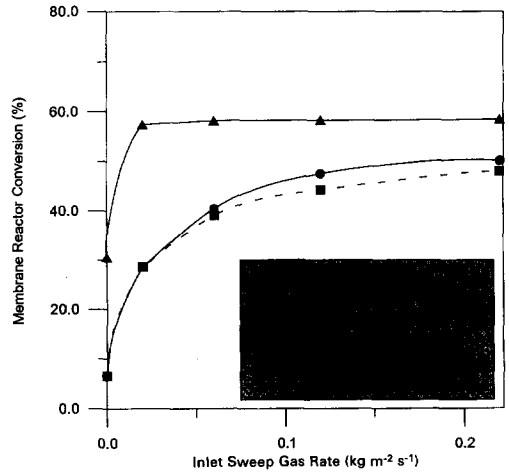

Fig. 8. Membrane reactor conversion vs inlet sweep gas rate. Inlet feed rate = 7.5×10^{-3} kg·m^{-2}·s^{-1}. Inlet temperature on both sides: $T = 490$ K.

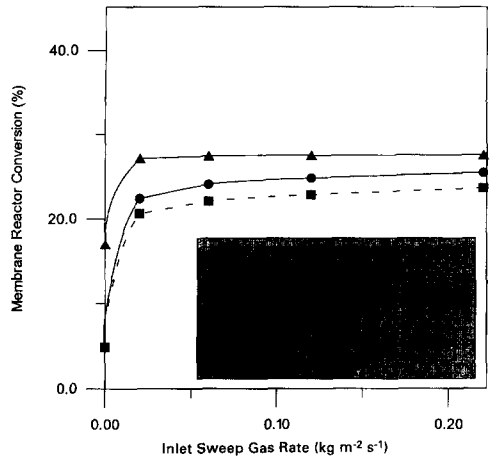

Fig. 9. Membrane reactor conversion vs inlet sweep gas rate. Inlet feed rate = 12.5×10^{-3} kg·m^{-2}·s^{-1}. Inlet temperature on both sides: $T = 470$ K.

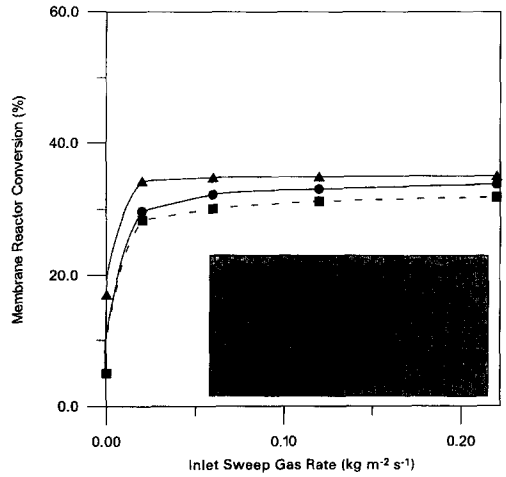

Fig. 10. Membrane reactor conversion vs inlet sweep gas rate. Inlet feed rate = 7.5×10^{-3} kg·m^{-2}·s^{-1}. Inlet temperature on both sides: $T = 470$ K.

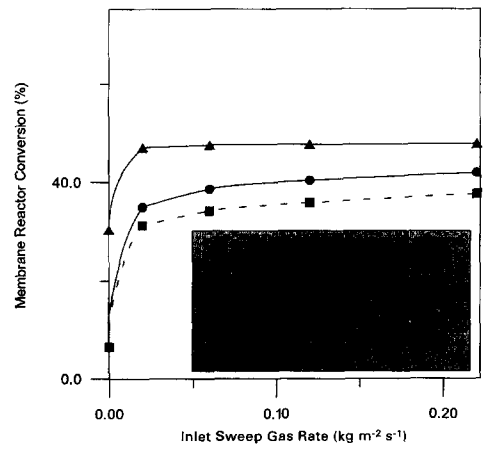

Fig. 11. Membrane reactor conversion vs inlet sweep gas rate. Inlet feed rate = 12.5×10^{-3} kg·m^{-2}·s^{-1}. Inlet temperature on both sides: $T = 490$ K.

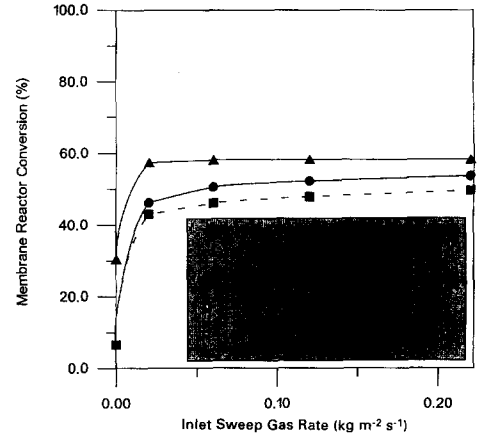

Fig. 12. Membrane reactor conversion vs inlet sweep gas rate. Inlet feed rate = 7.5×10^{-3} kg·m^{-2}·s^{-1}. Inlet temperature on both sides: $T = 490$ K.

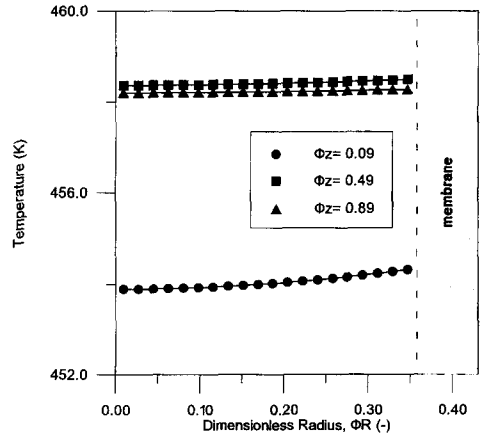

Fig. 13. Radial temperature profile on the feed side at three axial points. Adiabatic operation. $Q_f = 12.5 \times 10^{-3}$ kg·m^{-2}·s^{-1}, $Q_s = 1.2 \times 10^{-1}$ kg·m^{-2}·s^{-1}. Inlet temperature on both sides: $T = 470$ K. Heat dispersion model.

the outer membrane wall (Figs. 13–14) and radial heat dispersion effects are more intensive, in comparison with those on the feed side, where catalyst particles and fluid coexist. Thus, in the case of dispersion conditions, lower values of the membrane reactor conversion are predicted (in comparison with the case of the simplified model), as the quantity of heat transferred through the membrane decreases, inducing a lower shift of the equilibrium values (endothermic reaction).

In Figs. 15–16 typical axial temperature profiles on both sides of the reactor, in case of heat dispersion conditions, are presented. On the feed side, the temperature close to the reactor inlet decreases, reaching a minimum value, but then it increases along the axis to the outlet. This behaviour is easily explained considering the two heat effects that take place simultaneously: (i) heat consumption from the reaction; and (ii) heat transfer through the membrane from the separation side to the feed side.

An increase in inlet sweep gas temperature induces

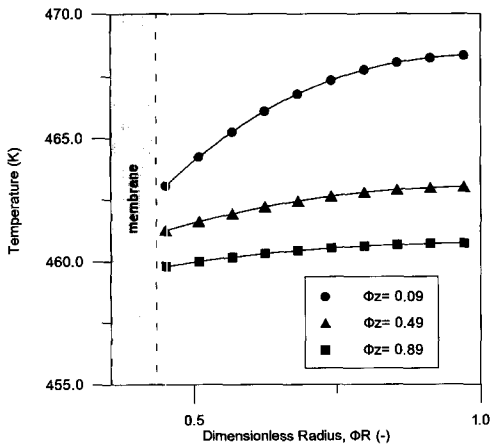

Fig. 14. Radial temperature profile on the separation side at three axial points. Adiabatic operation. $Q_f = 12.5 \times 10^{-3}$ kg·m^{-2}·s^{-1}, $Q_s = 1.2 \times 10^{-1}$ kg·m^{-2}·s^{-1}. Inlet temperature on both sides: $T = 470$ K. Heat dispersion model.

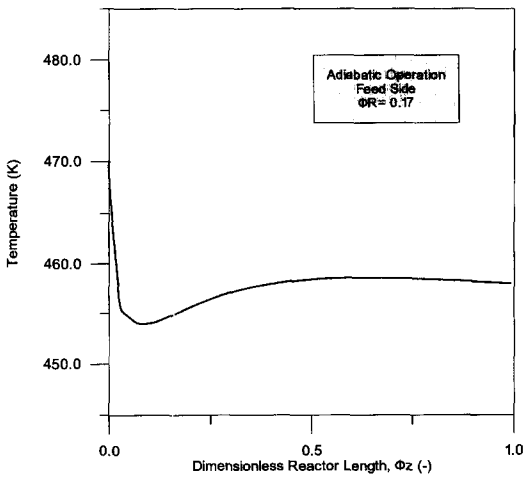

Fig. 15. Axial temperature profile on the feed side. $Q_f = 12.5 \times 10^{-3}$ kg·m^{-2}·s^{-1}, $Q_s = 1.2 \times 10^{-1}$ kg·m^{-2}·s^{-1}. Inlet temperature on both sides: $T = 470$ K. Heat dispersion model.

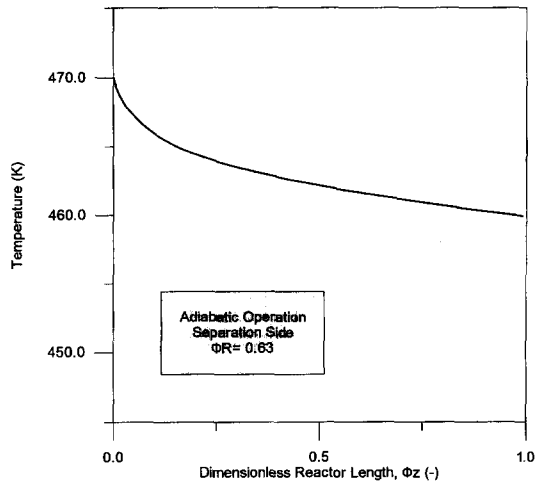

Fig. 16. Axial temperature profile on the separation side. $Q_f = 12.5 \times 10^{-3}$ kg·m^{-2}·s^{-1}, $Q_s = 1.2 \times 10^{-1}$ kg·m^{-2}·s^{-1}. Inlet temperature on both sides: $T = 470$ K. Heat dispersion model.

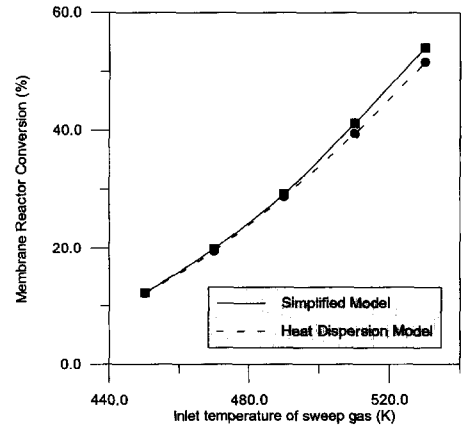

Fig. 17. Membrane reactor conversion vs inlet temperature of sweep gas. Inlet temperature on the feed side: $T = 490$ K. Inlet feed rate = 12.5×10^{-3} kg·m^{-2}·s^{-1}. Inlet sweep gas rate = 6×10^{-2} kg·m^{-2}·s^{-1}.

an increase in heat transfer through the membrane, and thus an increase in membrane reactor conversion because of the endothermic nature of the reaction (Fig. 17). Also, because of the latter reason, an increase in inlet feed temperature increases the reactor conversion (Figs. 5–12).

5. CONCLUDING REMARKS

This work focused on the development of a two-dimensional mathematical model for the simulation of the performance of a packed-bed membrane reactor under various operating conditions, taking into account the heat effects that take place inside the reactor.

The model is applied for the dehydrogenation of cyclohexane. Based on the results of the numerical simulation presented and analysed in this study, the conclusion drawn is that in the simulation of the performance of a membrane reactor, heat effects taking place inside the reactor have to be taken into account, because possible omission of them will induce an overestimation in the predicted temperature field and in the calculated reactor conversions.

Acknowledgements—The authors express their thanks to CHAM Ltd, London, UK, for permitting the use of their product PHOENICS. Also, they would like to acknowledge gratefully partial funding for this research work provided by the European Community.

REFERENCES

1. Sun, Y. M. and Khang, S. J. K., Catalytic membrane for simultaneous chemical reaction and separation applied to a dehydrogenation reaction. *Industrial Engineering Chemical Research*, 1988, **27**, 1136–1142.
2. Mohan, K. and Govind, R., Analysis of equilibrium shift in isothermal reactors with a permselective wall. *AIChE Journal*, 1988, **34**, 1493–1503.
3. Itoh, N., Shindo, Y., Haraya, K. and Hakuta, T., A

membrane reactor using microporous glass for shifting equilibrium of cyclohexane dehydrogenation. *Journal of Chemical Engineering Japan*, 1988, **21,** 399–404.
4. Hsieh, H. P., Inorganic membrane reactors. *Catalytic Review Science Engineering*, 1991, **33** (1&2), 1–70.
5. Edwards, M. F. and Richardson, J. F., Gas dispersion in packed beds. *Chemical Engineering Science*, 1968, **23,** 109–123.
6. Schlunder, E. U., On the mechanism of mass transfer in heterogenous systems in particular in fixed beds, fluidized beds and on bubble trays. *Chemical Engineering Science*, 1977, **32,** 845–851.
7. Froment, G. F. and Bischoff, K. B., *Chemical Reactor Analysis and Design*, 2nd edn. Wiley, New York, 1990, Chap. 11.
8. Wakao, N., Kaguei, S. and Funazkri, T., Effect of fluid dispersion coefficients on particle-to-fluid heat transfer coefficients in packed-beds-correlation of Nusselt numbers. *Chemical Engineering Science*, 1979, **34,** 325–336.
9. Spalding, D. B., Mathematical modelling of fluid mechanics, heat transfer and chemical reaction processes; a lecture course, HTS/80/1, Imperial College, London, 1980.
10. Patankar, S. V. and Spalding, D. B., A calculation procedure for heat, mass and momentum transfer in parabolic flows. *International Journal of Heat and Mass Transfer*, 1972, **15,** 1787–1806.
11. Markatos, N. C., Computational fluid flow capabilities and software. *Ironmaking and Steelmaking*, 1989, **16,** 266–273.
12. Markatos, N. C., Mathematical modelling of single- and two-phase flow problems in the process industries. *Revue de l'Institut Francais du Petrole*, 1993, **48** (6) 631–661.
13. Markatos, N. C. and Moult, A., The computation of steady and unsteady turbulent, chemically-reacting flows in axisymmetrical domains. *Transactions of the Institution of Chemical Engineers*, 1979, **57,** 156–162.
14. Spalding, D. B., A general purpose computer program for multi-dimensional one or two-phase flow. *Mathematical and Computers in Simulation*, 1981, **13,** 267–276.
15. Bird, R. B., Stewart, W. E. and Lightfoot, E. N., *Transport Phenomena*. Wiley, New York, 1960, Chap. 6.
16. Gunn, D. J. and Khalid, M. K., Thermal dispersion and wall heat transfer in packed beds. *Chemical Engineering Science*, 1975, **30,** 261–267.
17. Perry, R. H. and Green, D., *Perry's Chemical Engineers' Handbook*, 6th edn. McGraw-Hill, New York, 1984, Chap. 3.
18. Incropera, F. P. and De Witt, D. P., *Fundamentals of Heat and Mass Transfer*, 3rd edn. Wiley, New York, 1990, Chap. 8.
19. Reid, R. C., Prausnitz, J. M. and Sherwood, T. K., *The Properties of Gases and Liquids*, 3rd edn. McGraw-Hill, New York, 1977, Chap. 10.
20. Yagi, S., Kunii, D. and Wakao, N. *AIChE Journal*, 1960, **6,** 543–546.
21. Henley, E. J. and Seader, J. D., *Equilibrium-Stage Separation Operation in Chemical Engineering*. Wiley, New York, 1968.

APPENDIX 1: CALCULATION OF THERMAL PROPERTIES

(a) *The coefficient of heat transmission between the fluid on the feed side and the internal membrane surface*, h_f was calculated by the relation [16]:

$$h_f = 5 \cdot (\lambda_g/d_p) Re^{0.365}$$

where:

Re is the Reynolds number ($Re = \rho v_s d_p/\mu$)
ρ is the fluid density [kg m^{-3}]
μ is the viscosity of the fluid [Pa s]
d_p is the mean diameter of the catalyst particles [m]
v_s is the fluid axial superficial velocity [m s^{-1}]
λ_g is the heat conduction coefficient of the fluid [W m^{-1} K^{-1}].

(b) *The coefficient of transmission of heat between the fluid on the separation side and the external membrane surface*, h_s, was calculated by the relation [5]:

$$h_s = \lambda_g/D_h \cdot 1 \cdot 02 \cdot Re_{D_h}^{0.45} Pr^{0.5} (D_h/L)^{0.4} (D_3/D_2)^{0.8} Gr^{0.05}$$

where:

L is the reactor length [m]
D_2 is the diameter of the feed side + the membrane layer [m]
D_3 is the total diameter of the reactor [m]
D_h $= D_3 - D_2$
Re_{D_h} is the Reynolds number corresponding to equivalent diameter D_h
Gr is the Grashof number, given by: $Gr = L^3 \cdot \rho^2 \cdot g \cdot \beta \cdot \Delta t/\mu^2$ where g, is the gravity acceleration [m s^{-2}], $\beta = 1/T$ is the expansion factor [K^{-1}] and Δt, is the temperature difference causing the heat transfer (considered to be ~ 10 grads)
Pr is the Prandtl number ($= C_p \mu/\lambda_g$).

(c) *The coefficient of heat transmission between the fluid on the separation side and the external reactor wall*, h_s'. In the case of adiabatic performance, h_s' is zero. In the case of heat exchange between the fluid and the outer wall of the annulus, h_s' was calculated from the value of $Nu = 4.4$ [18].

(d) *The heat conduction coefficient of the fluid*, λ_g was calculated by the relation [W m^{-1} K^{-1}] [19]:

$$\lambda_g = \sum_{i=1}^{n} \left[x_i \lambda_{gi} \Big/ \left(\sum_{j=1}^{n} x_i A_{ij} \right) \right].$$

x_i are the molar fractions of the mixture components
λ_{gi} are individual heat conduction coefficients [W m^{-1} K^{-1}]

$$A_{ij} = /4\{1 + [(M_j/M_i)^{3/4} (T + S_i)/(T + S_j)]^{0.5}\}^2 \times (T + S_{ij})/(T + S_i)$$

M_i are the molecular weights of the components [kg gmol^{-1}]
T is the absolute temperature [K]
$S_i = 1.5 \cdot T_{bi}$ and $S_{ij} = (S_i \cdot S_j)^{0.5}$, where, T_{bi} are the normal boiling points of the components [K].

(e) *The radial effective heat dispersion coefficient on the feed side*, λ_{rf} was calculated by [7]:

$$\lambda_{rf} = \lambda_o + \lambda_{rt}$$

where:

λ_o is the effective heat conduction coefficient of the quiescent bed [W m^{-1} K^{-1}]
λ_{rt} is the dynamic contribution to the radial heat dispersion [W m^{-1} K^{-1}].

These are given as functions of the following parameters:

(i) $\lambda_o = f(\lambda_g, \varepsilon, \lambda_s)$ where ε, is the feed side porosity and λ_s, is the heat conduction coefficient of the solid particles [W m^{-1} K^{-1}] and
(ii) $\lambda_{rt} = f(\lambda_g, C_p, v_s, \rho, d_p, D_1)$, where D_1, is the inner tube diameter [m], v_s is the superficial axial velocity, C_p is the specific heat [J kg^{-1} K^{-1}], and d_p is the particle diameter [m].

(f) *The axial effective heat dispersion coefficient on the feed side*, λ_{af} was calculated by the relation [W m^{-1} K^{-1}] [8, 20]:

$$\lambda_{af} = \lambda_o + 0.7\rho C_p d_p u.$$

(g) *The axial and radial effective heat dispersion coefficient of the fluid on the separation side*, λ_{as}, λ_{rs} were calculated on the following basis. The heat dispersion is attributed exclusively to heat conduction inside the fluid, because of the low flow rate and the laminar flow mode and both the axial and the radial heat dispersion coefficients are assumed equal to the value of the heat conduction coefficient of the fluid, λ_g.

(h) *Specific heat of the fluid*, C_p. The mean specific heat of each component is calculated by the form [Btu lbmol^{-1} °F^{-1}]:

$$C_{pi} = A_{1i} + A_{2i}T + A_{3i}T^2$$

where the constants A_i are given below. The specific heat of the gas mixture is calculated by [J kg^{-1} K^{-1}]:

$$C_p = (4.19/\mathrm{MW})[\Sigma x_i A_{1i} + \Sigma x_i A_{2i} T + \Sigma x_i A_{3i} T^2]$$

where MW is the mixture mean molecular weight [kg gmol^{-1}].

Values of constant A_i used in the calculation of mean specific heat of each component [Btu lbmole^{-1} °F^{-1}] [21]

	A_1	A_2	A_3
Ar	4.96	0	0
C_6H_{12}	21.00	5.62×10^{-3}	1.13×10^{-5}
C_6H_6	16.39	4.02×10^{-1}	6.9×10^{-6}
H_2	6.64	2.5×10^{-3}	-4.5×10^{-6}

(i) *The heat of the reaction*, ΔH, was calculated by:

$$\Delta H = \Delta H_f^0 + \int_{298}^{T} \Sigma v_i \cdot C_{pi} \cdot dT$$

where:

ΔH_f^0 $= \Sigma H_f^0$ of products $- \Sigma H_f^0$ of reactants. The values of the enthalpies of formation are [kcal/gmol] [17]: H_2: 0.0, Ar: 0.0, C_6H_{12}: −29.43, C_6H_6: 19.82

H_f^0 is the enthalpy of formation of a compound (zero for an element) and

v_i are the coefficients of the components participating in the reaction (−1 for C_6H_{12}, 1 the C_6H_6 and 3 for H_2).